Erosion of a High-Carbon Steel in Coal and Bottom-Ash Slurries

O.P. Modi, Rupa Dasgupta, B.K. Prasad, A.K. Jha, A.H. Yegneswaran, and G. Dixit

(Submitted 3 February 2000)

This paper discusses the observations made during erosive wear testing of a high-carbon steel (0.65% C) in coal and bottom-ash slurries. The slurry was made by separately dispersing 30% coal and bottom ash (collected from a thermal power plant) in tap water. The tests were performed using a sample rotation method in the slurry at a fixed linear velocity of 5 m/s for different traversal distances at room temperature. To see the influence of microstructural features on slurry wear response, the steel was subjected to hardening and annealing heat treatments.

Test results indicate that material loss of the specimens increased with traversal distance in all cases. Further, the hardened steel showed a lower rate of material loss when compared with steel in an annealed condition in either of the test environments. Moreover, irrespective of heat-treatment conditions, the samples revealed significantly higher material loss when tested in the bottom-ash slurry than in the coal slurry. The higher rate of material removal in the case of the former was attributed to the more efficient transfer of the kinetic energy of the moving (hard) bottom-ash particles to the specimen surface than in the case of the softer coal particles. Fracture of coal particles as a result of impact during the course of slurry erosion further supported the view.

Results have been explained on the basis of the characteristics of the affected surfaces and changes in the morphology of the erodent particles after the test.

Keywords coal slurry, erosion, steel, surface engineering, wear

1. Introduction

Various machinery components used in mining, power generating, and civil and chemical engineering industries experience severe erosion leading to considerable material/production loss. In thermal power plants, pulverized coal is used as the fuel for generating electricity.[1,2,3] Indian noncoking coals supplied to thermal power stations contain 30 to 40% ash and even more. As is known, a very high quantity of (abrasive/erosive) quartz is present in the ash. A huge quantity of flyash/bottom ash, generated after burning coal in thermal power plants, is disposed off in the form of (water + ash) slurry into ash ponds.[1,2,3] This requires the use of pipes/tubes and other such components that suffer from severe problems of (slurry) erosion/abrasion of the components. Spraying of the water + coal slurry in thermal power generation industries[2,3] also leads to similar problems.

Factors such as composition, microstructure, and mechanical properties are some of the important factors that govern the wear resistance of steels.[4–10] Judicious selection of the composition and heat-treatment cycle leads to a significant improvement in the wear resistance property of steels.[11]

O.P. Modi, Rupa Dasgupta, B.K. Prasad, A.K. Jha, and **A.H. Yegneswaran**, Regional Research Laboratory (CSIR), Bhopal-462 026, India; and **G. Dixit**, Department of Applied Mechanics, Maulana Azad College of Technology, Bhopal-462 007, India. Contact e-mail: rrlabbpl@vsnl.com.

The erosion tests of a 304 stainless steel in coal and silica sand slurries carried out using a slurry jet impingement test at room temperature showed a significant increase in wear rate with the ash content in coal.[12–15] This has been explained to be due to the greater fracturing tendency of the coal and most effective transfer of the kinetic energy of sand particles to the target surface.[12–16] Similar observations have also been made in the case of rolled 1050 carbon steel tested in coal and alumina slurries.[15] However, very limited studies have been carried out on the erosive wear characteristics of steels in coal/bottom-ash slurries.[12–16] Further, there are conflicting observations regarding the effects of the microstructure of the specimens and the morphology and the nature of the erodent particles.[8,9,17] Moreover, the complexity of the erosive nature of a heterogeneous coal-containing dispersion of inorganic ash and pyrite in an organic matrix is not well understood.[12,13,14] The friability of coal could be an important property governing the severity of erosion/abrasion caused to the specimen surface. The role of the bottom ash containing a considerable amount of unburnt coal/carbon and α-quartz carries special significance, as it increases the severity of erosion/abrasion of the material.

With the above facts in mind, an attempt has been made in this study to examine the effects of changes in the microstructure and hardness of a 0.65% C steel brought about by two different heat-treatment cycles on its erosion behavior. Tests were carried out in water + 30% coal and water + 30% bottom-ash particle slurries. The influence of traversal distance on the erosion behavior of the steel in the slurries has also been examined. The observed response of the samples has also been substantiated through the examination of affected surfaces and the eroded particles after the tests.

Table 1 Heat-treatment cycles and hardness of steel

Serial number	Treatment	Hardness (Vickers)
1.	Annealing: austenitization at 900 °C for 1 h + furnace cooling	223
2.	Hardening: austenitization at 900 °C for 1 h + ice water quenching	738

Table 2 Proximate analysis of coal and bottom ash particles

Erodent particles	Moisture, %	Ash, %	Volatile matter, %	Fixed carbon, %
Coal	1.56	29.93	28.64	39.87
Bottom Ash	0.89	84.84	2.77	11.50

2. Experimental Procedures

2.1 Material

The steel selected in this study contained 0.65% C, 0.87% Mn, 2% Si, and balance Fe with equivalent carbon content being 0.7%. Accordingly, the steel can be termed as near eutectoid.

2.2 Heat Treatment and Hardness Measurement

Specimens (size: 10 × 5 × 1 cm) were cut from long steel plates and subjected to annealing and hardening heat treatments in a microprocessor-based electric muffle furnace. Annealing and hardening treatments were performed on the samples to produce two different kinds of microstructures. The treatment cycles and the bulk hardness values resulting from the corresponding treatment are shown in Table 1. Hardness of the specimens was determined on metallographically polished specimens using a Brinell-cum-Vickers hardness test apparatus at an applied load of 15 kg. An average of five observations has been reported in this study.

2.3 Size Analysis of Erodent Particles

Size analysis of run-of-mine (ROM) noncoking coal and bottom-ash (erodent) particles was performed on Augsburg, Germany make Apline Air Jet Sievers (Augsburg, Germany). The majority of coal particles in this case were in the size range of 150 to 500 μm. Further, the majority of the bottom-ash particles were observed to be in the size range of 150 to 300 μm.

2.4 Proximate Analysis

Table 2 shows the proximate analysis of the ROM noncoking coal and bottom-ash particles carried out using standard techniques.

X-ray diffraction studies conducted for coal and bottom-ash particles revealed the presence of phases such as carbon, kavlinite, and quartz in the case of coal samples, whereas quartz was the major phase and there were minor phases such as aluminum silicate, iron oxide, and rutile in the bottom ash.

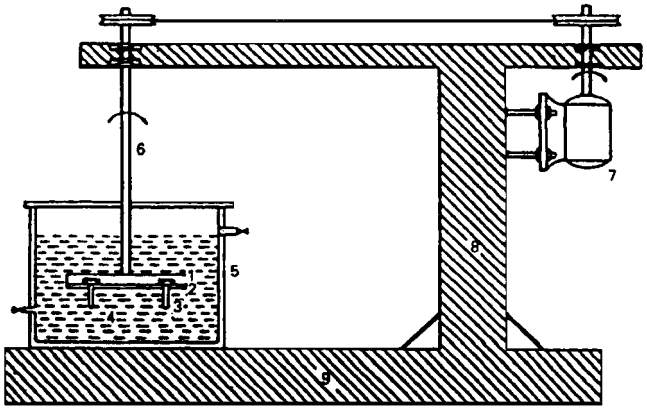

1: disc; 2: specimen holder; 3: specimen; 4: slurry media; 5: double wall container; 6: spindle; 7: driving motor; 8: column; 9: machine base

Fig. 1 A schematic diagram of slurry erosion/abrasion test apparatus

2.5 Slurry Wear Tests

Slurry wear tests were performed on metallographically polished samples with the help of a DUCOM (Bangalore, India), India-made slurry abrasion test apparatus using a sample rotation test method[18] at ambient temperature. A schematic diagram of the test apparatus is shown in Fig. 1. The test equipment essentially comprised a stainless-steel container holding the slurry wherein the specimen rotates. The specimens (size: 15 × 12 × 6 mm) were fixed onto a metallic disc at a fixed radial distance of 8 cm corresponding to a linear sliding distance of 0.5 m in every rotation. The disc assembly containing the specimens was rotated about its vertical axis in the tank containing the slurry with the help of an electric motor (Fig. 1).

The test was conducted at a rotational speed of 600 rpm corresponding to a linear velocity of 5.0 m/s in the slurries of water + 30% ROM noncoking coal and water + 30% bottom ash. The wear tests were performed at various test intervals such as 1, 2, 3, 5, 10, 15, 20, 25, and 30 h, corresponding to traversal distances of 18, 36, 54, 90, 180, 270, 360, 450, and 540 km. Tested specimens were rinsed with a copious amount of tap water followed by chemical cleaning as per ASTM standards.[19] The specimens were finally dried and weighed after ultrasonic cleaning in an acetone bath. Wear rates were computed by a weight loss technique. In view of variation in sample size, normalized wear rates in terms of volume loss per unit sliding distance per unit sample (initial) weight (mm^3/m/gm) were computed. Each experiment was repeated three times and an average taken to minimize the contribution of random error in measuring erosion rates.

2.6 Microscopy

The specimens (size: 10 × 10 × 10 mm) for microstructural examinations were prepared using standard metallographic techniques and etched with 2% Nital. The etched specimens were microstructurally examined using optical microscopy and scanning electron microscopy (SEM).

The worn surfaces of typical specimens were examined under SEM. The erodent particles were examined using SEM prior to and after the slurry tests. The particles were mounted on a brass stud for the purpose. All the specimens were sputtered with gold prior to their SEM examination.

3. Results

3.1 Microstructure

Microstructural features of the samples in annealed and hardened conditions are shown in Fig. 2. The annealed sample revealed the presence of pearlite and ferrite (Fig. 2a). The SEM micrograph clearly shows the presence of the lamellae of pearlite (Fig. 2b). Figure 2(c) shows the microstructure of the hardened sample to contain needle-shaped martensite.

3.2 Slurry Erosive Wear Behavior

The influence of traversal distance on the weight loss per unit area of the steel samples tested in water + 30% coal and water + 30% bottom-ash slurries is shown in Fig. 3. The influence of heat treatment on the erosion characteristics of steel can also be seen in the figure. The weight loss of the specimens increased with traversal distance in all cases (Fig. 3). The rate of increase in material loss was significantly high in the beginning (stage I). This was followed by a reduced rate in material loss (stage II) with a further increase in traversal distance. When the traversal distance was further increased, the specimens attained a steady-state wear condition (stage III). It may be noted that the extent of material loss was significantly larger in the case of annealed steel as compared to the hardened one irrespective of the test environments (Fig. 3). The steel samples both in hardened and annealed conditions experienced lower weight loss in the coal slurry than in the slurry of bottom ash (Fig. 3). The nature of the curve on the influence of distance traversed on weight loss was identical in the steel subjected to either of the heat-treatment cycles. The trends in the weight loss on both the slurry environments were also found to be similar (Fig. 3). Further, the difference in weight loss of the annealed samples tested in coal and bottom-ash slurries was reduced at longer traversal distances (Fig. 3).

The variation in the wear rate (computed from weight loss versus traversal distance curve) of the samples with distance traversed in coal and bottom-ash slurries is shown in Fig. 4. It may be seen that the wear rate increased initially with traversal distance (Stage I: acceleration period) and attained a peak value and then decreased at larger traversal distances (Stage II: deceleration period) in both the test environments. When the traversal distance was still longer, the stage of steady-state wear rate (Stage III) was achieved. No incubation period was noticed irrespective of test conditions adopted in the present study (Fig. 4). The wear rate corresponding to the peak value was found to be significantly higher in the case of specimens tested in the bottom-ash slurry when compared with the coal slurry. Further, the traversal distance corresponding to the peak value was found to be significantly lower when the tests were conducted in the bottom-ash slurry as compared to the coal slurry (Fig. 4). Moreover, the traversal distance corresponding to the peak value was observed to be significantly higher in the case of annealed steel when compared with the hardened steel in either of the test environments (Fig. 4).

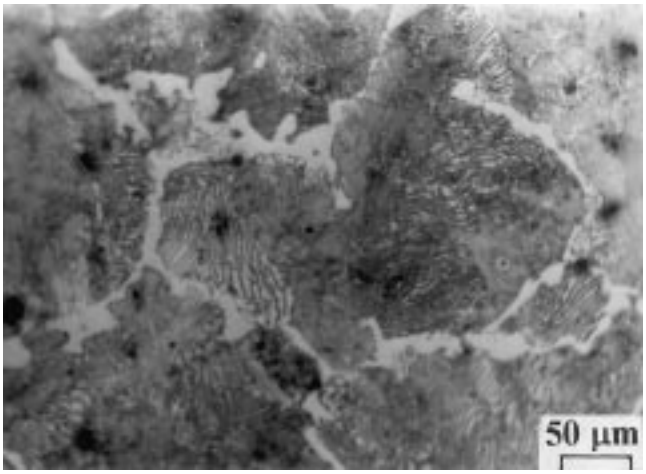

(**a**)

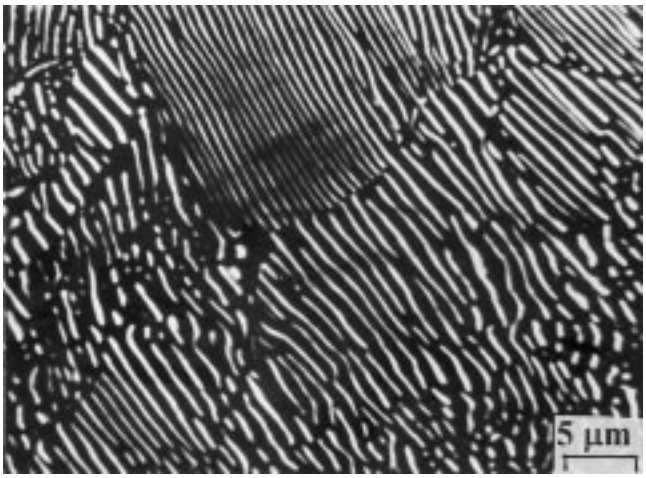

(**b**)

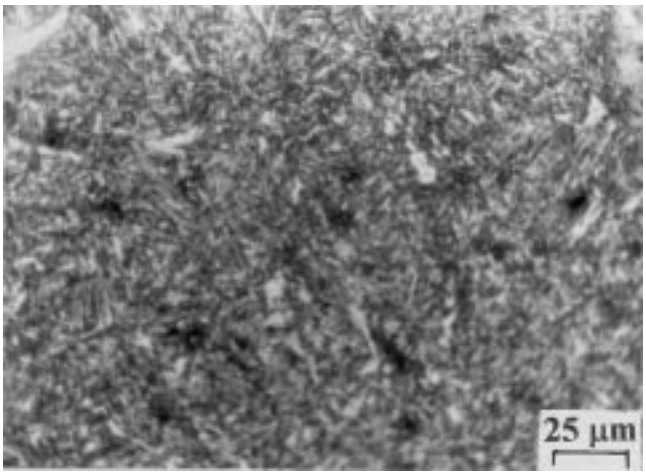

(**c**)

Fig. 2 Microstructural features of (**a**) and (**b**) annealed steel showing (a) pearlitic structure with ferrite network and (b) pearlite lamellae, and (**c**) hardened steel revealing martensitic structure

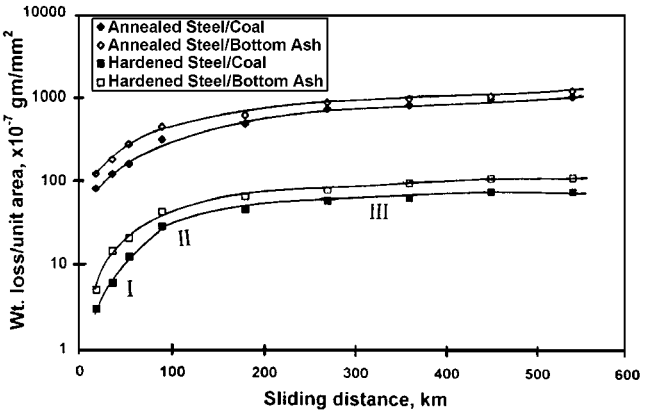

Fig. 3 Weight loss as a function of traversal distance of the steel in annealed and hardened conditions in the slurries of water + 30% coal and water + 30% bottom-ash particles at 5 ms^{-1}

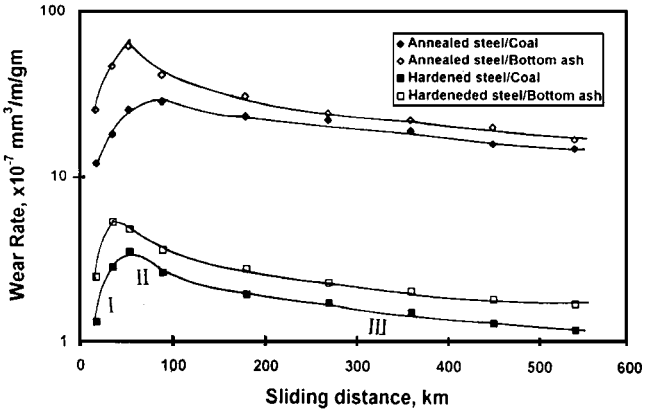

Fig. 4 Variation of wear rate with traversal distance of the annealed and hardened steels in water + 30% coal and water + 30% bottom-ash slurry environments at 5 ms^{-1}

(**a**)

(**b**)

Fig. 5 Eroded surfaces of steel in (**a**) annealed and (**b**) hardened conditions, exposed to water + coal slurry

3.3 Microscopic Study of Eroded Surfaces

The worn surfaces of the annealed and hardened steels after exposure for 30 h (~540 km traversal distance) in the slurry of coal and bottom ash are shown in Fig. 5 and 6. The worn surface of annealed steel in the slurry containing coal was characterized by shallow abrasion grooves and large-size erosion pits (Fig. 5a). Under the similar experimental condition, in the case of hardened steel, the abrasion marks were relatively deeper and there was the presence of significantly much smaller erosion pits (Fig. 5b). For annealed steel tested in a slurry of bottom ash, the worn surface was characterized by deep abrasion grooves with large-size erosion pits (Fig. 6a), whereas for hardened steel under the identical experimental condition, the abrasion grooves were more frequent with fewer erosion pits (Fig. 6b).

3.4 Morphology of Erodent Material

Morphology of erodent particles before and after slurry erosion tests is shown in Fig. 7 and 8. The fresh (a and b) as well as spent (c and d) coal particles showed the same degree of angularity (Fig. 7). In addition, the slurry-tested coal particles revealed a considerable reduction in size (Fig. 7c). A higher magnification micrograph of used coal particles clearly indicates the presence of a large number of cracks and a more uneven surface (Fig. 6d). Fresh bottom-ash particles were noted to be spherical in shape (Fig. 8a and b). The presence of micropores on the surface of the particles can also be seen in the figures. The slurry-tested bottom-ash particles revealed much less fracturing tendency after conducting the tests (Fig. 8c and d) as compared to coal particles (Fig. 7c and d).

4. Discussion

Material loss in a slurry medium takes place through the erosive action of the droplets of the liquid, which are formed due to relative motion between the slurry and the sample. A slurry known to contain suspended solid particles in a liquid impinges onto the sample surface and enhances the degree of material loss further. Material-related parameters (*e.g.*, material

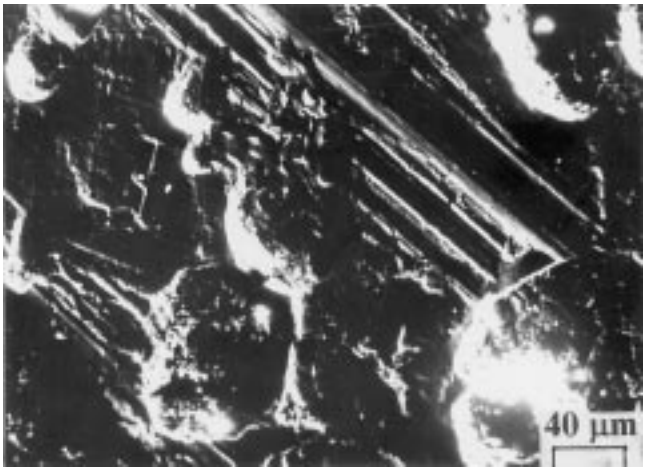

(**a**)

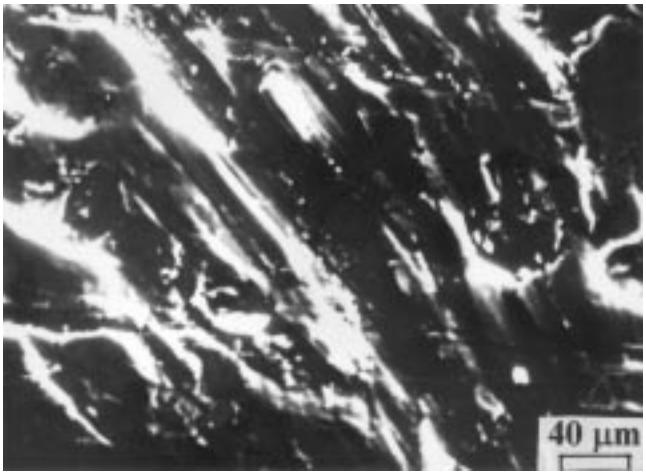

(**b**)

Fig. 6 Eroded surfaces of steel in (**a**) annealed and (**b**) hardened conditions, exposed to water + bottom-ash slurries

composition, microstructure, and hardness) and experimental variables (*e.g.*, nature of the medium, temperature, the flow conditions, the presence of entrance solid particles, and their shape, size, content, hardness, and surface contour) greatly control the erosion response of material.[20–23] Another important property of the eroding particles that has a significant effect is their physical integrity during their impingement on the specimen surface (*i.e.*, shatter resistance). During impact, if the eroding particles shatter, the resulting small pieces may not have the kinetic energy necessary to cause enough plastic deformation on the specimen surface. Further, the angular particles have greater ability to cause a higher extent of material erosion as compared to the rounded particles. This is very much the situation in the case of water + erodent (coal/bottom ash) slurries wherein the main damage to the specimen surface is through the impinging action of the slurry.[24]

A relative motion between the fluid and the specimen occurs in slurry through the rotation of the specimens in a fluid kept in a container. This results in the vortex formation in the solution causing entrapment of gas into the fluid system. The impingement of vortex causes mechanical damage to the specimen surface as a result of cavitation.

Considering the mechanisms of material removal for ductile and brittle materials, it emerges that ductile materials are eroded by a mechanism that sequentially extrudes, pancake forges, and finally fractures platelets of material off the target surface.[24] These features are observed in the large-shaped erosion pits, as shown in Fig. 5(a) and 6(a).

The increase in weight loss of the specimens with traversal distance in either of the slurry environments (Fig. 3) could be explained as due to the removal of the iron oxide scale from the steel surface due to the impinging action of the slurry erodent particles followed by the exposure of fresh metallic surface to the slurry environments. This leads to a continuous attack of the slurry on the specimen surface. Once the oxide layer breaks, the impact of the erodent particles on the steel surface causes a continuous increase in weight loss (Fig. 3).

Both annealed and hardened steel samples revealed lower wear loss in coal-containing slurry when compared with the slurry containing suspended particles of bottom ash (Fig. 3). This could be attributed to the poorer cutting property of the (relatively) softer coal particles[16] than the bottom-ash particles. Further, it is to be noted that, if the indenting particles (Fig. 7a) shatter during the process of erosion, the resulting small pieces (Fig. 7c) may not have the kinetic energy necessary to cause maximum plastic deformation of the target metal because a part of the energy associated with the particles is consumed in their fragmentation itself. Accordingly, in the case of the coal slurry, only a part of the total kinetic energy associated with the suspended coal particles is utilized for causing erosion of the steel samples.[14] This is evident from Fig. 5 and 6, where relatively more surface damage is seen in the case of steel tested in a slurry of bottom ash (Fig. 6a and b) as compared to the steel tested in a slurry of coal (Fig. 5a and b). The morphology of the coal erodent after the test shows a greater extent of fragmentation into small particles (Fig. 7c) with a larger number of microcracks on the surface (Fig. 7d) as compared to bottom-ash particles (Fig. 8c and d). The higher erosiveness of bottom-ash particles could be attributed to the presence of a variety of hard (mineral) constituents such as quartz, aluminum silicate, iron oxide, and titanium dioxide in much larger quantity than in coal. The higher material loss in the slurry of bottom ash than coal could be further substantiated with a greater Miller number (directly proportional to the erosiveness of slurry) in the case of the former.[25] The high wear loss of annealed steel (consisting of pearlitic structure with a small amount of ferrite network) as compared to the hardened steel (of martensitic structure) in either of the slurry media could be explained as due to the greater hardness of the hardened steel as compared to annealed steel (Fig. 3). This is also evident in the eroded surfaces of the steel where more abrasion damage (less material loss) is observed in the hardened steel (Fig. 5b and 6b) as compared to that of annealed steel (Fig. 5a and 6a) characterized by erosion pits (more material loss). This is true for both test environments (Fig. 5 and 6).

The varying degree of material loss during slurry wear occurs in four stages over the entire test duration/distance traversed.[26]

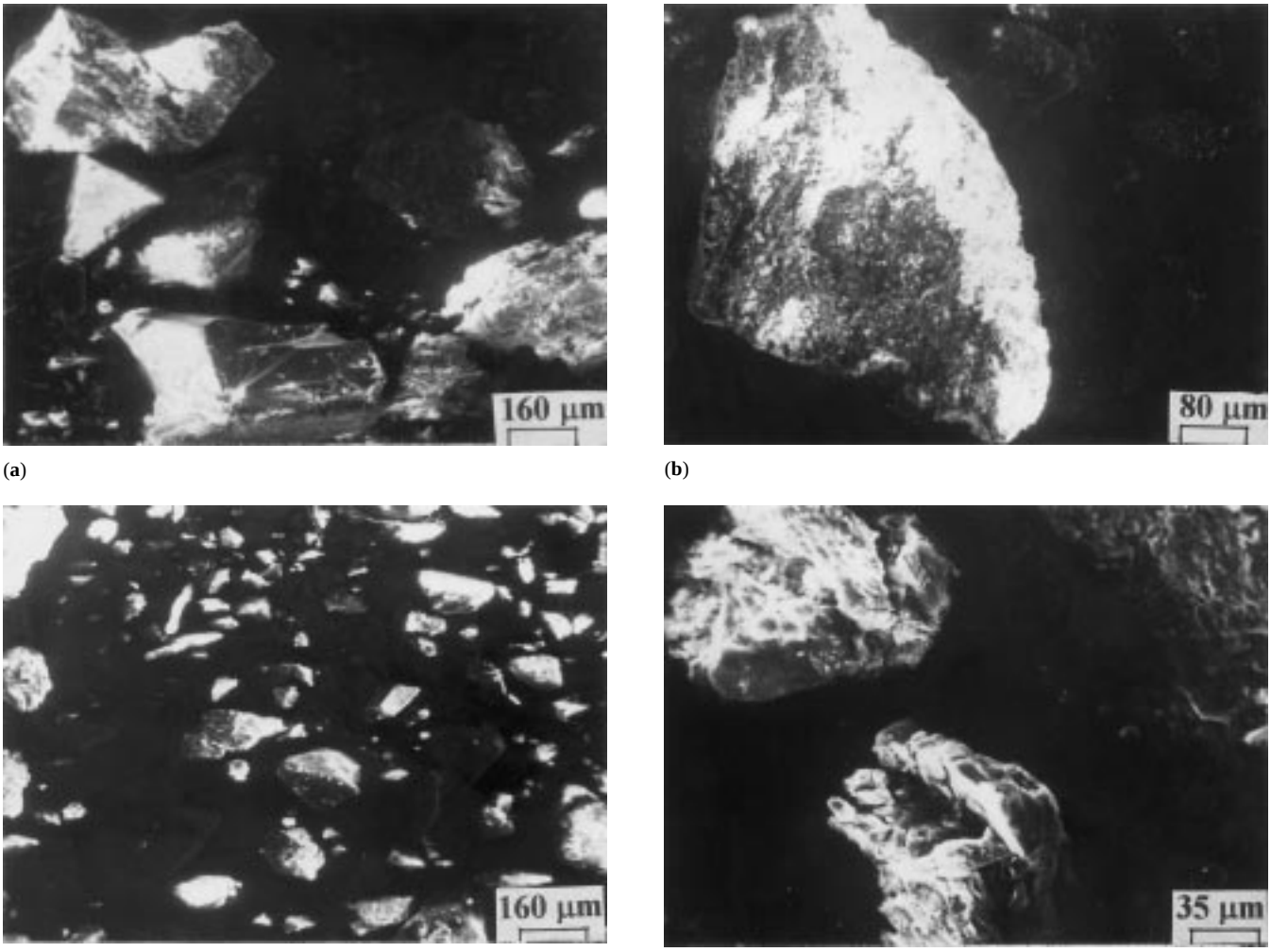

Fig. 7 Scanning electron micrographs of coal particles (**a**) and (**b**) before and (**c**) and (**d**) after slurry test

These four different stages are (1) incubation period, (2) accelerated erosion, (3) decelerated rate of material loss, and (4) steady-state wear rate. The incubation period (until the breaking of the oxide layer) could not be observed in the present study, since this period became too short to be observed when the first observation was made. The disintegration of the film grows into crater-like depressions on the surface of the material due to repeated plastic deformation,[27] developing smooth-edged pits on the metal surface. With increasing time/distance, the extent of pitting increases, resulting in enhanced rate of material loss.[27] The attainment of peak was caused by the nucleation of deep craters.[26] This results in a faster rate of material loss (Fig. 4). The entrapment of gas bubbles (generated by turbulence in the liquid) in the craters reduces the extent of direct contact of the medium with the metal surface. This causes reduced (decelerated) wear rate (Fig. 4). A counterbalancing effect of the increased material loss by deeper crater formation and reduction in wear rate due to entrapped gas bubbles in craters leads to the attainment of a steady-state wear rate.[28] The blunting action of the erodent particles in the slurry also gives rise to a reduction in material loss in the later stages.[26] Another reason for the lower rate of material removal in the final stage (*i.e.*, steady-state wear rate condition) could be attributed to the work hardening of the target material by the erodent particles.[28]

5. Conclusions

- The wear loss of the specimens increased with traversal distance in all cases.
- Higher material loss in steel samples in the bottom-ash slurry than in the coal slurry has been caused by the presence of a larger quantity of harder mineral constituents and less fracturing tendency of the former.
- The steel in the annealed condition revealed nearly ten times more material loss than the steel subjected to the hardening treatment in both slurry environments studied because of a more severe attack by the slurry on the softer annealed steel.

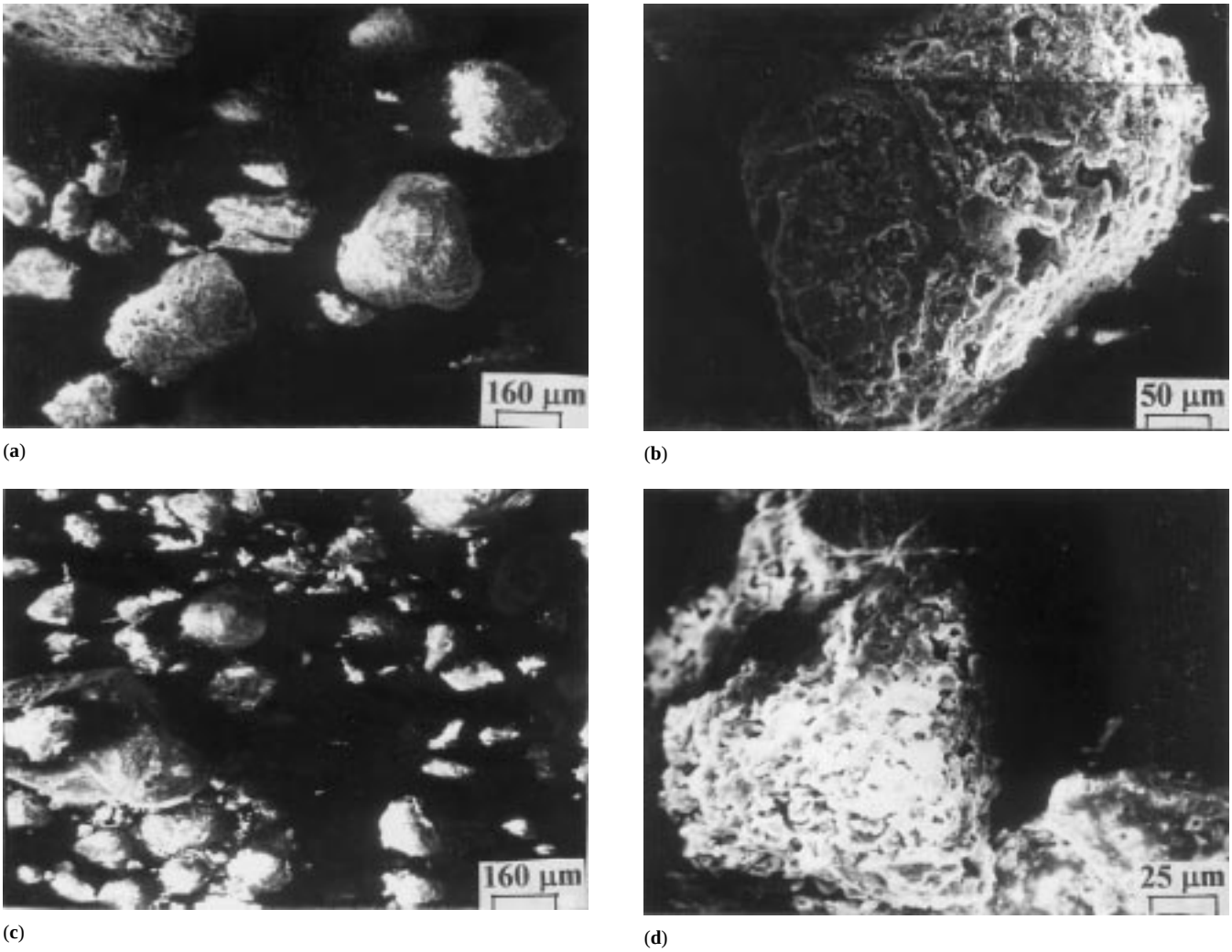

(**a**) (**b**) (**c**) (**d**)

Fig. 8 Scanning electron micrographs of bottom-ash particles (**a**) and (**b**) before and (**c**) and (**d**) after slurry test

Acknowledgments

The authors are thankful to Professor T.C. Rao, Director, Regional Research Laboratory (CSIR), Bhopal, for giving permission to publish this paper.

References

1. S. Mukhopadhay, G.K. Ganguly, and S. Dasgupta: *Ind. Mining Eng. J.*, 1999, Jan., pp. 27-33.
2. Technical Report No. 80, Central Board of Irrigation and Power, Maliha Marg, Chankyapuri, New Delhi, May 1992.
3. J.P. Burnwal: *Proc. Nat. Workshop on Materials Related Aspects of Thermal Power Plants*, jointly organized by Indian Institute of Metals, Regional Research Laboratory, and Madhya Pradesh Council of Science and Technology, 1996, at Regional Research Laboratory (CSIR), Bhopal - 462 026, India, published by IIM, Bhopal, India, pp. 1-8.
4. D.S. Sarma: *J. Tool Alloy Steels (India)*, 1993, Dec., pp. 395-407.
5. A.V. Levy and S. Jahanmir: in *Corrosion-Erosion Behaviour of Materials*, K. Natesan, ed., TMS-AIME, Warrendale, PA, 1979, p. 177.
6. I. Finnie, J. Wolak, and Y. Kabil: *J. Mater. Sci.*, 1967, vol. 2 pp. 682-702.
7. B.K. Prasad and S.V. Prasad: *Wear*, 1991, vol. 151, pp. 1-12.
8. J. Larsen Badse: *Scripta Metall.*, 1990, vol. 24, p. 821.
9. P.L. Hurricks: *Wear*, 1973, vol. 26, p. 285.
10. M.A. Moore: *Wear*, 1974, vol. 28, p. 59.
11. *Metals Handbook*, 9th ed., ASM, Metals Park, OH, 1985, vol. 1, pp. 597-638.
12. D.K. Spencer and A.A. Sagues: *Proc. Corrosion-Erosion Wear of Materials at Elevated Temperatures*, Berkeley, CA, 1986, A.V. Levy, ed., NACE, Publication, Berkeley, CA, 1986, pp. 367-84.
13. F.W. Bauer: *2nd Ann. Pittsburgh Coal Conf.*, 1985, Store and Webster Engineering Corp., 1985, TP 85-93, YB/CSG.
14. E. Raask: *Proc. 5th Int. Conf. on Erosion by Solid and Liquid Impacts*, Cavendish Laboratory, University of Cambridge, 1979, pp. 4101-07.
15. G.A. Sargent, D.K. Spencer, and A.A. Sagues: *Conf. Proc. Corrosion-Erosion: Wear of Materials in Engineering Fossil Energy Systems*, A. Levy, ed., NACE Publications, Houston, TX, 1982, pp. 196-221.
16. S. Hersheng, C. Huahul, and X. Xiaodi: *Int. Conf. on Tribology in Mineral Extraction*, Int. Mechanical Engineering Conf. publication 1984-II, Mechanical Engineering Publications Ltd., London, 1984, p. 35.
17. O. Scheffler and C. Allen: *Tribol. Int.*, 1988, vol. 21, p. 127.
18. O.P. Modi, B.K. Prasad, S. Das, A.K. Jha, and A.H. Yegneswaran: *Mater. Trans. JIM*, 1994, vol. 35, pp. 67-73.
19. F.H. Cocks: *Manual of Industrial Corrosion: Standards and Control*, ASTM, Philadelphia, PA, 1973, p. 262.

20. S. Turenne, Y. Chatigny, D. Simrad, S. Caron, and J. Masounave: *Wear*, 1990, vol. 141, pp. 147-58.
21. S. Turenne, D. Simrad, and M. Fiset: *Wear*, 1991, vol. 149, pp. 187-97.
22. R. Dasgupta, B.K. Prasad, A.K. Jha, O.P. Modi, S. Das, and A.H. Yegneswaran: *Mater. Trans. JIM*, 1988, vol. 39, pp. 1185-90.
23. R. Dasgupta, B.K. Prasad, A.K. Jha, O.P. Modi, S. Das, and A.H. Yegneswaran: *Wear*, 1997, vol. 213, pp. 41-46.
24. A. Levy: *Corrosion*, 1995, vol. 51, pp. 872-83.
25. A.W. Ruff and S.M. Wiederhorn: *Treatise on Materials Science and Technology*, vol. 16, *Erosion*, C.M. Preece, ed., Academic Press, New York, NY, 1979.
26. O.P. Modi, B.K. Prasad, R. Dasgupta, A.K. Jha, and D.P. Mondal: *Mater. Sci. Technol.*, 1999, vol. 15, pp. 933-38.
27. J.B. Zu, G.T. Burstein, and I.M. Hutchings: *Wear*, 1991, vol. 149, pp. 73-84.
28. M.K. Aghajanian, M.A. Rocazella, J.T. Burke, and S.D. Keck: *J. Mater. Sci.*, 1991, vol. 26, pp. 447-54.